Environmental Science & Technology

Article

pubs.acs.org/est

Nitrogen Isotope Composition of Thermally Produced NO_x from Various Fossil-Fuel Combustion Sources

Wendell W. Walters,[*,†] Bruce D. Tharp,[‡] Huan Fang,[†] Brian J. Kozak,[§] and Greg Michalski[†,‡]

[†]Department of Earth, Atmospheric, and Planetary Sciences, Purdue University, 550 Stadium Mall Drive, West Lafayette, Indiana 47907, United States

[‡]Department of Chemistry, Purdue University, 560 Oval Drive, West Lafayette, Indiana 47907, United States

[§]Department of Aviation Technology, Purdue University, 1401 Aviation Drive, West Lafayette, Indiana 47907, United States

Supporting Information

ABSTRACT: The nitrogen stable isotope composition of NO_x (δ^{15}N-NO_x) may be a useful indicator for NO_x source partitioning, which would help constrain NO_x source contributions in nitrogen deposition studies. However, there is large uncertainty in the δ^{15}N-NO_x values for anthropogenic sources other than on-road vehicles and coal-fired energy generating units. To this end, this study presents a broad analysis of δ^{15}N-NO_x from several fossil-fuel combustion sources that includes: airplanes, gasoline-powered vehicles not equipped with a three-way catalytic converter, lawn equipment, utility vehicles, urban buses, semitrucks, residential gas furnaces, and natural-gas-fired power plants. A relatively large range of δ^{15}N-NO_x values was measured from −28.1‰ to 8.5‰ for individual exhaust/flue samples that generally tended to be negative due to the kinetic isotope effect associated with thermal NO_x production. A negative correlation between NO_x concentrations and δ^{15}N-NO_x for fossil-fuel combustion sources equipped with selective catalytic reducers was observed, suggesting that the catalytic reduction of NO_x increases δ^{15}N-NO_x values relative to the NO_x produced through fossil-fuel combustion processes. Combining the δ^{15}N-NO_x measured in this study with previous published values, a δ^{15}N-NO_x regional and seasonal isoscape was constructed for the contiguous U.S., which demonstrates seasonal and regional importance of various NO_x sources.

INTRODUCTION

Nitrogen oxides (NO_x = NO + NO_2) are trace gases that play several important roles in tropospheric chemistry.[1,2] NO_x controls the photochemical production of ozone, a tropospheric oxidant and greenhouse gas, and influences the concentration of the hydroxyl radical, which acts as the detergent of the atmosphere, removing carbon monoxide, methane, and volatile organic compounds.[3] Oxidation of NO_x leads to the formation of nitric acid (HNO_3), which is subsequently deposited via wet and/or dry deposition leading to the acidification of the environment.[4] The major sources of NO_x are soil emissions, biomass burning, lightning, and fossil-fuel combustion,[4,5] and since the industrial revolution, anthropogenic NO_x emissions have surpassed natural NO_x emissions.[4,5] However, the NO_x emission budget is regionally and seasonally variable and differs significantly between remote and urban areas.[6,7] In order to estimate the relative importance of various NO_x sources in local/regional nitrogen (N) deposition, source identification and apportionment of NO_x and their oxidized products are required.

Once emitted into the atmosphere, NO_x primarily oxidizes to particulate nitrate (p-NO_3^-) and HNO_3; therefore, analysis of their N stable isotope ratio ($^{15}N/^{14}N$) might be a useful tool for partitioning NO_x sources or reactivity.[8−10] Previous measurements of the nitrogen stable isotope composition of NO_x (δ^{15}N-NO_x; $\delta^{15}N(‰) = [(^{15}N/^{14}N)_{sample}/(^{15}N/^{14}N)_{air} - 1] \times 1000$, where air N_2 is the N isotopic reference) have indicated a rather large range for various NO_x sources (Figure 1).[10−22] Whether these large ranges of δ^{15}N-NO_x are due to actual variations within a source or from differences in measurement methodology is not entirely clear.[19] For example, vehicle δ^{15}N-NO_x has been characterized to range from −13‰ to 17‰.[10,12,16,18,20,23,24] We recently performed an extensive study on NO_x emitted directly from vehicle tailpipes and found δ^{15}N-NO_x to range from −15.1‰ to 10.5‰ that negatively correlated with the emitted NO_x concentration and vehicle run time.[18] This trend was hypothesized to be the result of thermal NO_x production that is depleted in $^{15}NO_x$ abundance and subsequent NO_x reduction by three-way catalytic converters that increases $\delta^{15}NO_x$ abundance as a function of reduction efficiency.[18] Vehicle δ^{15}N-NO_x higher

Received: June 5, 2015
Revised: August 27, 2015
Accepted: September 2, 2015

DOI: 10.1021/acs.est.5b02769
Environ. Sci. Technol. XXXX, XXX, XXX−XXX

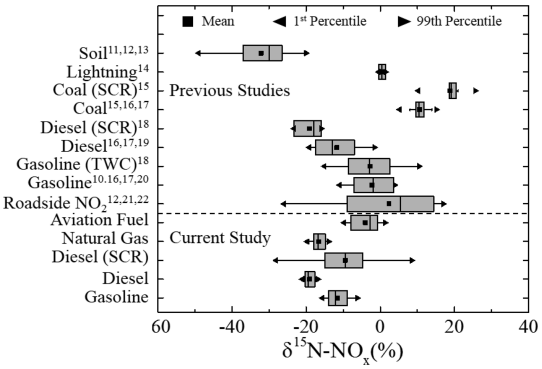

Figure 1. Box and whisker plot summarizing the distribution (lower extreme, lower quartile, median, upper quartile, and upper extreme) of δ^{15}N-NO_x previously measured[10−22] and reported in this study for various NO_x sources and fuel types. Presence of catalytic NO_x reduction technology is indicated by SCR (selective catalytic reducer) and TWC (three-way catalytic converter).

than 10.5‰ was not determined from NO_x emitted directly from vehicle tailpipes. Instead, they were inferred from δ^{15}N in roadside plant material,[21−23] tree rings,[24] and roadside NO_2.[12,21,22] Since these measurements are the δ^{15}N of a secondary product formed from vehicle-emitted NO_x, the measured δ^{15}N may be subject to kinetic and equilibrium isotope effects that can alter the original δ^{15}N-NO_x emitted from vehicles.[10,25,26] Therefore, further characterization of δ^{15}N-NO_x emitted directly from NO_x sources is required to minimize uncertainty in current published values to help assess the utility of δ^{15}N-NO_3^- as a NO_x source or chemistry tracer.

The variation of δ^{15}N-NO_x for different combustion sources may be related to the mechanism in which NO_x is produced.[27,28] The production of NO_x from combustion processes can be classified into two general categories either "thermal NO_x" or "fuel NO_x".[27−29] Thermal NO_x forms due to the thermal fixation of atmospheric N_2, while fuel NO_x forms due to the oxidation of chemically bound nitrogen within the fuel.[27−29] The majority of NO_x production in transportation related combustion sources originates from the thermal production, as the N content in gasoline, diesel, aviation fuel, and natural gas is negligible.[27,28,30−33] Thermal NO_x production occurs through four main mechanisms: the extended Zeldovich mechanism, the "prompt" mechanism, the nitrous oxide (N_2O) mechanism, and the NNH intermediate mechanism.[31,34,35] The prevalence of these mechanisms depends on the combustion conditions such as temperature, pressure, and amount of oxygen present in the combustion chamber.[31] Regardless of the mechanism, the N source for the thermally produced NO_x is air ($\delta^{15}N_{air}$ = 0‰); consequently, it was first thought that combustion NO_x would be close to δ^{15}N = 0‰.[10,16] However, direct δ^{15}N-NO_x measurements of thermally produced NO_x tend to be negative (Figure 1).[16,18,19] The depletion in $^{15}NO_x$ abundance is likely due to the kinetic isotope effect associated with the breaking of the triple bond of N_2 that favors the dissociation of $^{14}N^{14}N$ over $^{15}N^{14}N$, due to $^{14}N^{14}N$ having a higher zero point energy (1175.7 cm^{-1}) than $^{15}N^{14}N$ (1156.0 cm^{-1}).[36] Previously, we have estimated the δ^{15}N-NO_x associated with the extended Zeldovich mechanism (the dominant mechanism for NO_x production in vehicles)[37] using a harmonic oscillator approximation for relative reaction rates for the formation of ^{14}NO and ^{15}NO to be approximately −9.5‰.[18] Presumably, other mechanisms for the thermal NO_x production will also emit NO_x depleted in ^{15}N, because in each case a N bond must break, which will favor the dissociation of ^{14}N over ^{15}N. However, the exact N fractionation for the various thermal NO_x production pathways may be slightly different due to the pathway's reaction energetics and temperature since the magnitude of an isotopic fractionation is temperature dependent.[38]

The characterization of δ^{15}N-NO_x emitted directly from fossil-fuel combustion sources has improved in recent years, but uncertainties remain.[10,15,16,18−20] It has been suggested that anthropogenic NO_x emission sources have δ^{15}N-NO_x values close to zero or that are positive,[10,39] but this may not be true for all anthropogenic NO_x sources, since production of thermal NO_x results in negative δ^{15}N-NO_x values.[18] The presence of NO_x reduction technology (i.e., three-way catalytic converters), though, appears to increase δ^{15}N-NO_x values relative to the produced NO_x as observed in vehicles[18] and in coal-fired power plants.[15] The magnitude of this δ^{15}N-NO_x increase, however, is not clear for all NO_x sources, and in many cases, combustion engines are not equipped with catalytic NO_x reduction technology. To the best of our knowledge, there is no δ^{15}N-NO_x data for fossil-fuel combustion sources that make up a significant percentage of the NO_x emission budget of the U.S. and can have limited NO_x reduction capabilities. These include: aircraft (0.7%), off-road diesel-powered engines and equipment (8%), off-road gasoline-powered engines and equipment (2%), natural gas-burning EGUs (8%), and on-road heavy duty diesel-powered engines (17%).[40] In this study, we measured the N isotopic composition in these fossil-fuel combustion sources.

MATERIALS AND METHODS

NO_x Collection and Processing. Exhaust grab samples were collected from 19 different fossil-fuel combustion sources that included: three airplanes, two gasoline-powered vehicles not equipped with a three-way catalytic converter, five gasoline-powered lawn tools, one 4 × 4 utility vehicle, three diesel-electric urban buses, three diesel semitrucks, one residential gas furnace, and one natural gas-fired power plant. Samples were collected near West Lafayette, IN, U.S. (40.45° N, 86.91° W), Lafayette, IN, U.S. (40.42° N, 86.88° W), and La Plata, MD, U.S. (38.53° N, 76.97° W) between October 1, 2014 and May 1, 2015 using a modification of the U.S. Environmental Protection Agency Method 7.[41] Briefly, exhaust or flue samples were collected into a 2 L borosilicate bottle evacuated to 75 Torr. The sampling bottles contained 10 mL of a NO_x absorbing solution that was prepared by diluting 2.8 mL of concentrated sulfuric acid (H_2SO_4) and 0.6 mL of 30% hydrogen peroxide (H_2O_2) to 1 L using Millipore water.[41] The absorbing solution quantitatively oxidizes NO_x into NO_3^-.[41] Isotope effects associated with diffusion fractionation or collection of NO_x in ambient air are negligible in our NO_x grab sample setup.[18] Between 3 and 12 replicate samples were collected for each combustion source usually as a function of engine run time. Seven fossil-fuel combustion sources were equipped with either pre- or postcombustion NO_x reduction technology. Both the natural gas residential furnace and power plant were equipped with low-NO_x burners, a type of precombustion NO_x reduction technology that limits the formation of NO_x,[42] and three urban buses and two semitrucks sampled had selective catalytic reducers (SCR), a type of postcombustion catalytic NO_x reduction technology. Prior to collection, the various combustion sources were typically warmed up between 1 and 5 min. Details for each combustion

DOI: 10.1021/acs.est.5b02769
Environ. Sci. Technol. XXXX, XXX, XXX−XXX

Table 1. Fossil-Fuel Combustion Source Details, NO_x Concentrations, and $\delta^{15}N$-NO_x Values for Collected Exhaust or Flue Samples

NO_x source	fuel type	NO_x reduction technology	run time prior to sampling (min)	sector assignment	$\bar{x}$-NO_x (ppm)[a]	σ-NO_x (ppm)[b]	$\bar{x}$-$\delta^{15}N$ (‰)[a]	σ-$\delta^{15}N$ (‰)[b]	n (replicates)
Airplane 1 (Idle)	Aviation Gasoline	No	4	Mobile: Airplane	39	10	−7.5	3	4
Airplane 1 (Throttle)	Aviation Gasoline	No	10	Mobile: Airplane	185	50	−7.7	0.4	4
Airplane 2	Aviation Gasoline	No	4	Mobile: Airplane	456	60	0.6	1	4
Airplane 3	Aviation Gasoline	No	4	Mobile: Airplane	462	95	−1.5	0.7	4
1976 BMW 2002	Gasoline	No	5	Mobile: Gasoline Light Duty	63	7	−13.6	1	11
1972 Dodge Challenger Rallye	Gasoline	No	5	Mobile: Gasoline Light Duty	71	13	−9.5	1	5
Bobcat 3400 4x4 UTV	Gasoline	No	60	Mobile: Off-Road Gasoline Light Duty	30	5	−7.6	1	5
Urban Bus 1	Diesel-Electric	Post: SCR	1	Mobile: Diesel Heavy Duty	160	40	−20.9	7	4
Urban Bus 2	Diesel	Post: SCR	3	Mobile: Diesel Heavy Duty	146	20	−15.7	2	4
Urban Bus 3	Diesel-Electric	Post: SCR	180	Mobile: Diesel Heavy Duty	32	4	−1.7	3	4
Semi-Truck 1	Diesel	No	3	Mobile: Diesel Heavy Duty	160	20	−19.1	2	5
Semi-Truck 2	Diesel	Post: SCR	4.5	Mobile: Diesel Heavy Duty	24	10	−2.0	8	6
Semi-Truck 3	Diesel	Post: SCR	5	Mobile: Diesel Heavy Duty7	45	23	−10.9	3	4
STIHL Leaf Blower	Gasoline	No	5	Off-Road: Gasoline Engines/Equipment	132	40	−14.3	1	8
STIHL Yard Trimmer	Gasoline	No	5	Off-Road: Gasoline Engines/Equipment	80	30	−9.6	1	7
John Deere 2303 Tractor	Gasoline	No	5	Off-Road: Gasoline Engines/Equipment	141	15	−14.6	1	4
Troy Bilt Mode Tuff Cut 210	Gasoline	No	5	Off-Road:Gasoline Engines/Equipment	47	10	−10.7	1	3
Craftsman DTY400 Tractor	Gasoline	No	5	Off-Road: Gasoline Engines/Equipment	31	1	−8.5	0.3	3
Residential Furnace	Natural Gas	Pre: Low-NO_x Burner	5	Fuel Combustion: Electric Generation	34	10	−15.5	1	12
Power Plant	Natural Gas	Pre: Low-NO_x Burner	N/A	Fuel Combustion: Residential Heating	70	10	−17.9	1	11

[a]$\bar{x}$ = mean. [b]σ = standard deviation.

source (i.e., fuel type, NO_x reduction technology, and warm-up time) can be found in Table 1, and a more specific description for the collection procedure for each combustion source can be found in the Supporting Information.

After sampling, the exhaust/flue gases collected within the bottles were equilibrated with the NO_x absorbing solution for at least 72 h with occasional shaking every 10 to 12 h to facilitate the conversion of NO_x to NO_3^-. Residual NO_x headspace concentrations were measured using a chemiluminescence NO−NO_2−NO_x analyzer (Thermo-Environmental Instrument), and the NO_x absorbing solution was collected and neutralized using 1 mL of 1 M sodium bicarbonate buffer. The converted NO_3^- concentrations were measured using a UV−vis spectrometer (Cary 5000), and the percent of NO_x conversion to NO_3^- was calculated on the basis of the residual NO_x and converted NO_3^- concentrations. In each case, at least 99.3% of all collected NO_x was converted to NO_3^-, suggesting that N isotopic fractionation during this conversion should be minimized. Control tests indicate that the NO_3^- blank in the NO_x absorbing solution was below the detection limit. Recently, the presence of ammonia (NH_3) has been suggested as a possible interference in NO_x absorbing solutions specifically those that use potassium permanganate ($KMnO_4$) which will slowly oxidize NH_3 to NO_3^- under basic conditions.[19] This was tested as a possible interference by adding NH_3 into the employed NO_x absorbing solution. No detectable NO_3^- formed even at relatively high ammonium (NH_4^+) concentrations (100 ppm) and a wait time of one month, which is the longest time the solutions sat before being analyzed for $\delta^{15}N$. Therefore, we believe that NH_3 has a minimal to no impact on either the measured NO_3^- concentrations or the $\delta^{15}N$-NO_x values. Control tests using NO and NO_2 of a known isotopic composition that went through the entire NO_x collection procedure indicate that the reproducibility in our measured $\delta^{15}N$-NO_x values is ±1.3‰.

Isotopic Analysis. N isotopic analysis was carried out on the product NO_3^- in the absorption solution. Approximately 250 nmoles of NO_3^- was injected into a 12 mL vial containing 1 mL of a denitrifying strain of bacteria (*P. aureofaciens*) that lacks the nitrous oxide (N_2O) reductase enzyme, converting NO_3^- into nitrous oxide (N_2O).[43] The N_2O was extracted and purified using an automated head space gas chromatography system and analyzed by a Thermo Delta V Continuous Flow Isotope Ratio Mass Spectrometer (CF-IRMS) for m/z 44, 45,

DOI: 10.1021/acs.est.5b02769
Environ. Sci. Technol. XXXX, XXX, XXX−XXX

and 46 at the Purdue Stable Isotopes Lab.[44] Working lab standards, calibrated to NIST isotope reference nitrates USGS34 and USGS35, were used to correct for isotopic fractionation resulting from the denitrification of NO_3^- and the subsequent N_2O purification process. The working standards had an average standard deviation of 0.3‰ for $\delta^{15}N$.

RESULTS AND DISCUSSION

Table 1 details the data measured from the various fossil-fuel combustion sources. The text below summarizes the measured $\delta^{15}N\text{-}NO_x$ values of the collected samples and discusses our interpretation of these results and possible implications. The $\delta^{15}N\text{-}NO_x$ values measured for the various fossil-fuel combustion sources are summarized in Figure 1 sorted by fuel type.

Thermal NO_x $\delta^{15}N$ Values. The $\delta^{15}N\text{-}NO_x$ values for most of the combustion sources appear to be associated with the production of thermal NO_x. Excluding the NO_x sources equipped with an SCR (Table 1), the average $\delta^{15}N\text{-}NO_x$ for each source tended to be negative, ranging from −19.1‰ to 0.6‰, indicating that these samples generally had less $^{15}NO_x$ abundance than the N isotopic reference N (air). Within any given source, the standard deviations ranged from 0.3‰ to 3‰. This $\delta^{15}N\text{-}NO_x$ range is consistent with previous isotopic measurements of NO_x collected from the tailpipes of vehicles without catalytic converters (−13‰ to −2‰)[16] and exhaust samples collected from a diesel engine in a smog chamber (−18.0 ± 1)‰.[19] Negative $\delta^{15}N$ values in NO_x produced by vehicles with cold-engines, when NO_x catalytic reduction is inefficient, have also been observed.[18] All together, this suggests that thermally produced NO_x tends to be depleted in ^{15}N abundance.

The fuel type and engine design may have played a role in the $\delta^{15}N\text{-}NO_x$ emitted by different combustion sources (Figure 1). The gasoline-powered combustion engines that included light duty vehicles, lawn equipment/tools, and a utility vehicle had an average $\delta^{15}N\text{-}NO_x$ of −11.5‰ ± 2.7‰ (n = 46). This average $\delta^{15}N\text{-}NO_x$ is within one standard deviation of our predicted value for the extended Zeldovich mechanism of −9.5‰.[18] In contrast, the average $\delta^{15}N\text{-}NO_x$ for diesel sources without SCR was −19.1‰ ± 1.8‰ (n = 5) and −16.5‰ ± 1.7‰ (n = 33) for natural gas combustion sources (power plant and residential furnace), which were significantly lower than gasoline-powered sources (p < 0.01). Both gasoline and diesel combustion engines generally produce NO_x through the extended Zeldovich mechanism during the peak-temperature phase when temperatures exceed 2000 K;[45,46] therefore, N fractionation associated with the temperature that NO forms likely cannot explain the observed difference in $\delta^{15}N\text{-}NO_x$. We hypothesize that the observed difference may be related to the significance of NO decomposition in the combustion chamber. During the peak-temperature phase, NO concentrations reach a maximum, but NO subsequently decomposes postcombustion due to high temperature reactions with N, O, and H radicals.[45,47] In diesel engines, combustion gases cool more quickly postcombustion than in gasoline engines due to mixing of high temperature gas with air or cooler burned gases, which does not occur in gasoline engines.[45] Consequently, less NO decomposition occurs in diesel engines compared to gasoline engines.[45] If NO decomposition reactions are kinetically controlled, then they will occur faster for ^{14}NO than for ^{15}NO, and this would lead to the enrichment of ^{15}NO. Thus, if NO decomposition was more significant in gasoline engines than for diesel engines, this would enrich ^{15}NO abundance in gasoline engines compared to diesel engines and may explain higher $\delta^{15}N\text{-}NO_x$ values in gasoline engines. However, other differences between gasoline and diesel engines such as air-to-fuel ratios, cylinder pressures, ignition timing, and exhaust gas recirculation rates may also play a role in the observed difference in $\delta^{15}N\text{-}NO_x$.[46]

Unlike gasoline and diesel engines, low-NO_x burner natural-gas combustion does not predominately produce NO_x through the extended Zeldovich mechanism.[48] The flames in low-NO_x burners natural-gas combustion have temperatures that have been measured to range from 800−1600 K,[49] but the extended Zeldovich mechanism is significant only at temperatures more than 1800 K because of its high activation energy (~76 kcal/mol).[31] Natural gas combustion models indicate that, below 1400 K, NO_x production occurs mainly through the N_2O and the NNH mechanism.[48] While it is difficult to estimate the N fractionation associated with the N_2O and NNH mechanism due to the complicated nature of these mechanisms, we expect the observed $\delta^{15}N\text{-}NO_x$ from natural-gas combustion to reflect the average contribution of the thermal NO_x production mechanism and their associated temperature dependent N fractionation. Thus, the difference between the $\delta^{15}N\text{-}NO_x$ values for gasoline and natural gas combustion sources is likely due to both the N_2O and NNH mechanism possibly having a different NO_x isotopic fractionation signature than the extended Zeldovich mechanism, as well as natural gas combusting at lower temperatures.

The other type of fuel used by combustion sources in this study was aviation fuel, which is a highly refined form of gasoline.[32,33] These samples (3 airplane piston engines) had an average $\delta^{15}N\text{-}NO_x$ of −4.0‰ ± 4.0‰ (n = 16). Interestingly, airplane 1, had an average $\delta^{15}N\text{-}NO_x$ of −7.6‰ ± 1.8‰ (n = 8), which is nearly within one standard deviation of our estimated value for the extended Zeldovich mechanism. Airplane 1 was sampled both at idle position and while under load, but no significant difference in $\delta^{15}N\text{-}NO_x$ was observed (p > 0.1; Table 1). However, both airplanes 2 and 3, which were both sampled while under load, had an average $\delta^{15}N\text{-}NO_x$ value of −0.45‰ ± 1.4‰ (n = 8). The $\delta^{15}N\text{-}NO_x$ values for airplanes 2 and 3 were statistically significantly higher than any other of the combustion sources analyzed in this study (p < 0.01). These two airplanes' $\delta^{15}N\text{-}NO_x$ values suggest isotope equilibrium, rather than kinetic isotope effects, might have been important. Theory predicts that the N isotopic exchange between N_2, O_2, and NO (R1) would result in $\delta^{15}N\text{-}NO_x$ of −0.9‰ at combustion temperatures of 2200 K.[50]

$$N_2 + O_2 \leftrightarrow 2NO \quad \text{(R1)}$$

This predicted value is within one standard deviation of the average $\delta^{15}N\text{-}NO_x$ emitted from airplanes 2 and 3, indicating that, under their combustion conditions, N isotopic equilibrium (R1) might have been reached.[16] Previously, Heaton[16] used isotopic equilibrium to explain high NO_x concentrations and $\delta^{15}N\text{-}NO_x$ values that were close to 0‰ for gasoline and diesel vehicles operating under heavy-load conditions when combustion temperatures are higher and reaction times are longer. Engine load may explain why airplanes 2 and 3 reached equilibrium, but airplane 1, while under load, did not seem to reach isotopic equilibrium based on its average $\delta^{15}N\text{-}NO_x$. While not entirely clear why two of the airplanes reached isotopic equilibrium unlike all other combustion engines in this study, in general, the thermal NO_x tends to be depleted in ^{15}N

DOI: 10.1021/acs.est.5b02769
Environ. Sci. Technol. XXXX, XXX, XXX−XXX

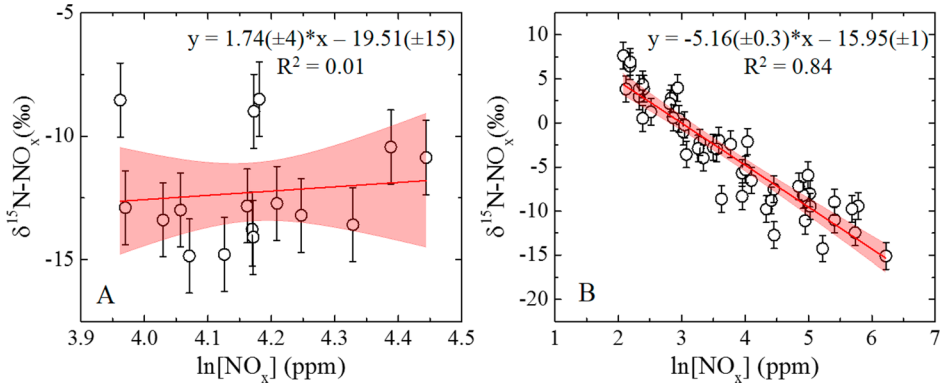

Figure 2. δ^{15}N-NO$_x$(‰) as a function of collected ln[NO$_x$] (ppm) for two gasoline-powered vehicles without (A) and with (B) a 3-way catalytic converter. (B) Adapted from ref 18. Copyright 2015 American Chemical Society. Linear fit is indicated by the red line, and the 95% confidence interval is shown in light red.

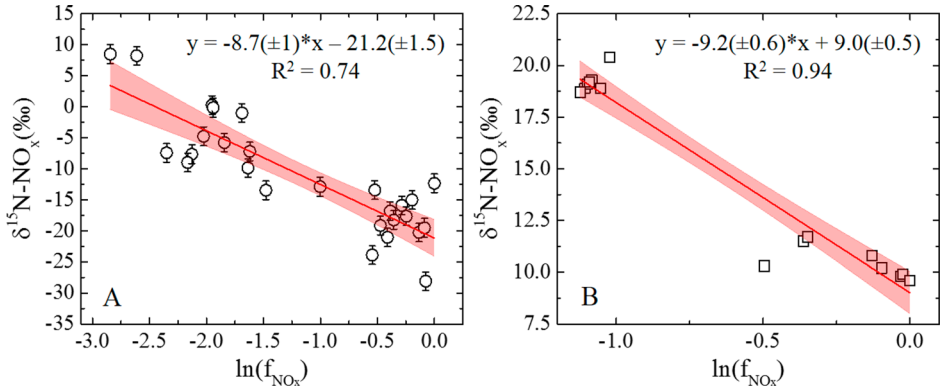

Figure 3. Impact of SCR technology on δ^{15}N-NO$_x$(‰) as a function of ln[f_{NOx}] where f_{NOx} is the fraction of NO$_x$ normalized to the highest [NO$_x$] emission for heavy-duty diesel-powered buses and trucks (A) and coal-fired power plants (B).[15] Linear fit is indicated by the red line, and the 95% confidence interval is shown in light red.

abundance with the magnitude of depletion dependent on combustion engine design and temperature. Further identification of the importance of N equilibrium isotope effects in combustion sources will need to be addressed in future δ^{15}N-NO$_x$ characterization studies.

Impact of Catalytic Reduction of NO$_x$ on δ^{15}N-NO$_x$. Our previous suggestion that catalytic reduction of NO$_x$ enriches ^{15}NO$_x$ abundance relative to the combustion produced NO$_x$ is supported by the data in this study.[18] In our previous study, there were no measurements of δ^{15}N-NO$_x$ produced by gasoline-powered vehicles not equipped with a three-way catalytic converter. In this study, we measured the δ^{15}N-NO$_x$ emitted from two vehicles without three-way catalytic converters. The δ^{15}N-NO$_x$ and NO$_x$ concentration emitted by these two vehicles were compared to vehicles equipped with three-way catalytic converters (Figure 2). Overall, the vehicles without catalytic converters emitted NO$_x$ with negative δ^{15}N-NO$_x$ values with low variation (−13.6 ± 1‰ and −9.5‰ ± 1‰) that did not correlate with the emitted NO$_x$ concentrations (R^2 = 0.01; Figure 2A). This is in contrast to gasoline-powered vehicles equipped with three-way catalytic converters that exhibited a strong correlation between NO$_x$ concentrations and δ^{15}N-NO$_x$ (R^2 = 0.84; Figure 2B). This supports our previous hypothesis that catalytic reduction of NO$_x$ increases δ^{15}N-NO$_x$ values relative to the thermally produced NO$_x$ during diffusion and absorption in the catalytic converter that favors ^{14}NO$_x$ reduction over ^{15}NO$_x$.[18]

A similar trend of increasing δ^{15}N-NO$_x$ with decreasing NO$_x$ concentrations was observed for heavy-duty diesel-powered engines equipped with SCR technology. Both heavy-duty diesel and diesel-electric powered engines emitted δ^{15}N-NO$_x$ that strongly correlated with the emitted NO$_x$ concentrations (R^2 = 0.74; Figure 3A). Generally, under cold-engine conditions, the emitted NO$_x$ concentrations were higher because of the inefficiency of SCRs at low temperatures,[51,52] and low δ^{15}N-NO$_x$ values reflected the predominance of thermal NO$_x$ (Figure 3A). As the converter warms up, the efficiency of the catalytic reduction of NO$_x$ increases, NO$_x$ emissions diminish,[51,52] and the catalytic reduction of NO$_x$ enriches ^{15}NO$_x$. In order to determine the δ^{15}N isotope enrichment factor associated with the catalytic reduction of NO$_x$ by diesel-powered engines equipped with SCRs, the process was modeled as a Rayleigh distillation process:

$$\delta^{15}N_{Reduced} = \delta^{15}N_{Thermal} + \varepsilon_{R/T}\ln[f_{NO_x}] \quad (1)$$

where $\delta^{15}N_{Reduced}$ is the measured δ^{15}N-NO$_x$ exiting the catalytic converter, $\delta^{15}N_{Thermal}$ is the δ^{15}N value of thermal NO$_x$ exiting the combustion chamber, f_{NOx} is the fraction of the thermal NO$_x$ remaining after catalytic reduction, and $\varepsilon_{R/T}$(‰) is the enrichment factor associated with catalytic NO$_x$ reduction (R) relative to the initial thermal NO$_x$ (T). From Figure 3A, $\varepsilon_{R/T}$ for the reduction of heavy-duty diesel-powered engines was calculated to be −8.7(±1)‰, which is close to the $\varepsilon_{R/T}$ previously calculated for light-duty diesel-powered engines of

DOI: 10.1021/acs.est.5b02769
Environ. Sci. Technol. XXXX, XXX, XXX−XXX

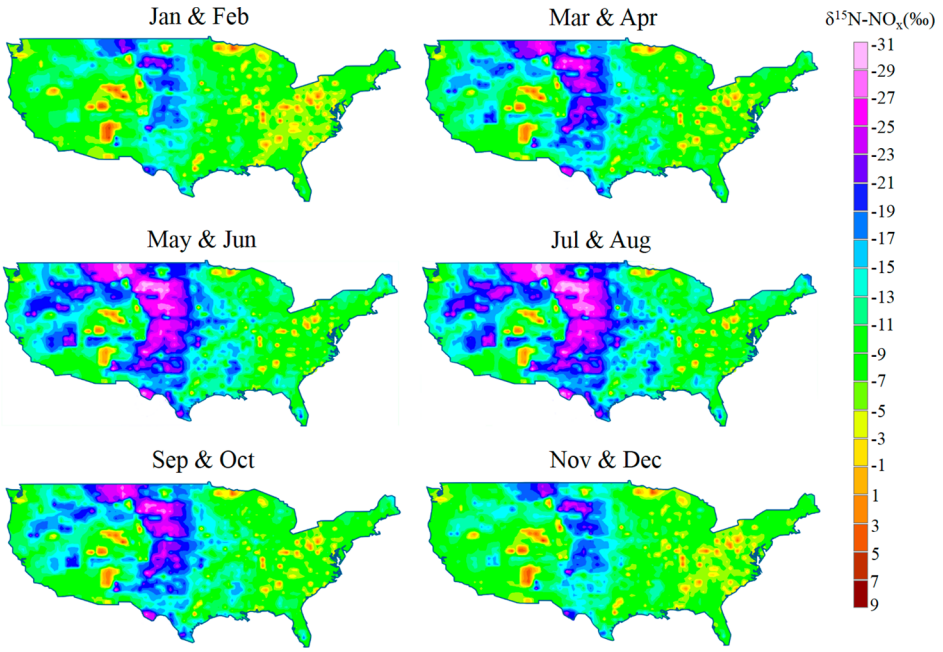

Figure 4. Bimonthly δ^{15}N-NO_x isoscape across the contiguous U.S.

−6.1(±0.8)‰.[18] Both the heavy and light-duty diesel-powered engines were equipped with SCR technology. In this catalytic system, liquid urea is injected into the exhaust pipeline leading to its vaporization and subsequent decomposition to NH_3. NH_3 is then absorbed on the surface of the catalytic converter and reacts with NO_x to form water and nitrogen.[46,53] Therefore, we hypothesize that the observed $\varepsilon_{R/T}$ could be due to the following isotopic fractionation processes: (1) NO diffusion through N_2 to the catalyst surface, (2) kinetic isotope effect associated with NO binding onto the surface of the metal catalyst, and/or (3) kinetic isotope effect of NO dissociating on the metal catalyst. To this end, we have calculated the following ε for these processes: (1) −7.8‰, (2) −16.3‰, and (3) −17.9‰ (full details on these calculations can be found in the Supporting Information). On the basis of these calculations, it appears that the observed fractionation is most likely due to rate limitation caused by NO diffusion through N_2.

Recently, the impact of SCR on δ^{15}N-NO_x in coal-fired power plants has been studied[15] and also indicates that SCR technology increases δ^{15}N-NO_x values. In order to determine the $\varepsilon_{R/T}$ associated with SCR technology in coal-fired power plants, we modeled the measured δ^{15}N-NO_x values for power-plant "D"[15] under conditions with SCR technology on and off and also as a Raleigh distillation process (eq 1; Figure 3B). This gives an $\varepsilon_{R/T}$ of −9.2‰ ± 0.6‰, which is within one standard deviation of the calculated value for SCR in heavy-duty diesel vehicles. This result suggests that similar NO_x reduction technologies involving catalysts are fractionating NO_x because of a diffusion layer near the catalytic surface resulting in comparable enrichment factors. While the $\varepsilon_{R/T}$ associated with SCR technology for both diesel-engines and coal-fired power plants seem to be similar, the absolute δ^{15}N-NO_x value associated with these two sources is quite different. In the absence of SCR technology, our model indicates that diesel engines would emit δ^{15}N-NO_x of −21.5‰ ± 1.5‰, while coal-fired power plants would emit δ^{15}N-NO_x of 9.0‰ ± 0.5‰ (Figure 3). The difference in these values can be explained by the NO_x production mechanism. In diesel engines, NO_x is produced thermally and, as previously discussed, favors the formation of $^{14}NO_x$ compared to $^{15}NO_x$, resulting in negative δ^{15}N-NO_x values. However, coal-fired power plant combustion temperatures (1550−1675 K) are too low for significant formation of thermally produced NO_x.[54] Instead, most of the NO_x is formed from the N derived from the coal as "fuel NO_x".[55] Coal has been measured to have δ^{15}N values of 1−1.2‰[16] and 2.0−2.2‰.[15] Our modeled value for the coal-fired power plant emitted δ^{15}N-NO_x is significantly higher than the δ^{15}N of the coal. This likely occurs due to the influence of postcombustion reactions involving the decomposition of NO that significantly lowers NO concentrations.[16] On the basis of the kinetic isotope effect, NO decomposition will occur faster for ^{14}NO than for ^{15}NO,[16] resulting in δ^{15}N-NO_x larger than the δ^{15}N of the coal.

Overall, the observed trend in the catalytic reduction of NO_x and δ^{15}N-NO_x is significant and suggests that regulated NO_x emissions (i.e., equipped catalytic NO_x reduction technology) from combustion sources has resulted in the gradual elevation of δ^{15}N-NO_x in the U.S. since the implementation of the Clean Air Acts.[56] This is suspected to occur since our data and previous studies[15,18] indicate that the catalytic reduction of NO_x increases δ^{15}N-NO_x values relative to the produced NO_x from fossil-fuel combustion sources. The magnitude of this elevation will depend on both the catalytic reduction technologies NO_x fractionation signature and the efficiency of the NO_x reduction. Thermally produced NO_x without catalytic NO_x reduction technology will tend to have negative δ^{15}N-NO_x values with the magnitude depending on engine design and combustion temperature conditions. This may allow for the prediction of δ^{15}N-NO_x from other NO_x sources, assuming that the majority of the NO_x originates from the thermal production and that the combustion temperature is known. To this end, we estimate that marine vessels and locomotives (both sources yet to be characterized for δ^{15}N-NO_x) that operate using diesel fuel will emit δ^{15}N-NO_x values close to −19‰ and those vessels equipped with SCR will emit δ^{15}N-NO_x values close to 0‰.

DOI: 10.1021/acs.est.5b02769
Environ. Sci. Technol. XXXX, XXX, XXX−XXX

Regional and Seasonal δ^{15}N-NO_x Variations. The δ^{15}N-NO_x inventory was used to predict the spatial and temporal variation of δ^{15}N-NO_x values across the contiguous U.S. The data obtained in this study, combined with other δ^{15}N-NO_x source characterization studies,[10−22] accounts for roughly 80% of all emitted NO_x in the contiguous U.S. based on 2011 U.S. EPA NO_x emission inventory.[40] The fraction of NO_x ($f_{source(i)}$) from each EPA source category was estimated at the county level using the 2011 EPA NO_x emission inventory.[40] The δ^{15}N-NO_x value for each source ($\delta^{15}N_{source(i)}$ and $f_{source(i)}$) was then used to solve the isotope mass balance equation for each county (eq 2).

$$(\delta^{15}\text{N-NO}_x)_{\text{total}} = \sum_i f_{\text{source}(i)} \times \delta^{15}\text{N}_{\text{source}(i)} \quad (2)$$

The total NO_x emission for each source by county from the 2011 U.S. EPA NO_x emission inventory was scaled for bimonthly NO_x emissions. The annual county NO_x totals for soil,[57] coal,[58] and natural gas[58] were apportioned on a monthly basis according to seasonal usage and soil emission estimates. All other NO_x sources were assumed to emit at a constant rate throughout the year. Bimonthly δ^{15}N-NO_x isoscapes for the contiguous U.S. were produced using ArcMap, and the inverse distance weighted (IDW) interpolation technique was applied between counties. The δ^{15}N-NO_x values used in the constructed isoscape and a full explanation of our seasonal NO_x source apportionment methods is provided in the Supporting Information.

Figure 4 stresses the regional dependency of δ^{15}N-NO_x based on the dominant NO_x emission source of the region. The high percentage of soil emissions over the Great Plains region and the low δ^{15}N-NO_x values of soil emissions resulted in this region typically having the lowest δ^{15}N-NO_x in the U.S. On the other hand, locations near coal-fired power plants have the highest δ^{15}N-NO_x as this source tends to have the highest δ^{15}N-NO_x.[15,16] Generally, the more polluted a region, the higher is the δ^{15}N-NO_x since the largest natural emissions (soil) have the lowest δ^{15}N-NO_x.[12,13] Additionally, Figure 4 shows the importance of seasons on the regional δ^{15}N-NO_x that are generally driven by soil emissions. During the summer, when soil emissions are largest,[57] lower δ^{15}N-NO_x values are predicted relative to the other months. Conversely, during the winter, δ^{15}N-NO_x values are highest because soil emissions are lowest since denitrification is limited at cold temperatures.[57] Seasonal variations in δ^{15}N-NO_x are not predicted in regions in which the major NO_x source contributor remains relatively unchanged throughout the year, such as regions dominated by vehicle NO_x emissions and power plants.

The predicted δ^{15}N-NO_x values for the contiguous U.S. were compared to observed δ^{15}N values in NO_x and NO_3^- in precipitation. Studies of δ^{15}N-NO_x from ambient air in the U.S. report values ranging from −24.6‰ to 7.3‰,[19,22] which is in excellent agreement with our δ^{15}N-NO_x isoscape model that has values ranging from −31‰ to 9.7‰. Measurements of the δ^{15}N-NO_3^- in wet and dry deposition, in the U.S., however, range from −9.5‰ to 14.1‰,[8,9,22] typically on the higher end of our predicted δ^{15}N-NO_x isoscape model. However, it is important to point out that the availability of both δ^{15}N-NO_x and δ^{15}N-NO_3^- data is exceedingly limited and mainly exists for the northeastern region of the U.S.[8,9,19,22] The discrepancy in the predicted δ^{15}N-NO_x and the measured δ^{15}N-NO_3^- in wet and/or dry deposition could be related to limited δ^{15}N-NO_3^- data or due to several other reasons. First, equilibrium isotope effects likely increase the δ^{15}N as NO_x is converted to NO_3^- prior to deposition.[25,26] The observed difference may then be associated with regional differences in NO_x oxidation pathways. Additionally, δ^{15}N may increase as NO is oxidized to NO_3^- due to dry deposition of NO and NO_2 which kinetically would favor the loss of ^{14}N. Alternatively, the discrepancy may be due to an incomplete assessment of δ^{15}N values from all NO_x sources. We note that the data obtained from this study have limited sample size and may not accurately represent the δ^{15}N-NO_x emitted from all types of gasoline, diesel, and natural gas fossil-fuel combustion sources. Similar types of studies in the future are necessary to reduce uncertainty in δ^{15}N-NO_x values.

While the exact causation of the alteration of δ^{15}N is beyond the scope of this work, if δ^{15}N-NO_3^- is linked to δ^{15}N-NO_x, Figure 4 suggests that (1) there are regional variations in δ^{15}N-NO_3^- based on the region's dominant NO_x source; (2) δ^{15}N-NO_x values may not be as high as previously thought,[39] and positive values generally only exist in regions with a significant amount of coal-fired NO_x emissions; (3) δ^{15}N-NO_3^- should reflect seasonal changes in areas where seasons affect the relative importance of NO_x sources; however, meteorological conditions may transport NO_x and NO_3^-, and this would alter measured δ^{15}N-NO_3^- compared to a regions emitted δ^{15}N-NO_x. Future studies should be directed toward further characterizing δ^{15}N-NO_x sources that include industrial processes, marine vessels, oil, and biomass-burning fossil fuel combustion, which represent approximately 8.5%, 2.9%, 1.9%, and 0.8% of all NO_x emission in the U.S., respectively.[40] Additionally, the impact of N fractionation processes due to chemical reactions and photolysis during the conversion of NO_x to NO_3^- needs to be better assessed and will be the subject for a future study.

■ ASSOCIATED CONTENT

Supporting Information

The Supporting Information is available free of charge on the ACS Publications website at DOI: 10.1021/acs.est.5b02769.

Appendix table, detailed sampling information, SCR enrichment factor calculations, δ^{15}N-NO_x values for isoscape (PDF)

■ AUTHOR INFORMATION

Corresponding Author

*E-mail: waltersw@purdue.edu. Phone: (765)-496-4906. Fax: (765)-496-1210.

Notes

The authors declare no competing financial interest.

■ ACKNOWLEDGMENTS

One of the authors (W.W.W.) was a National Science Foundation Graduate Research Fellow during the course of the study. We would like to thank the Purdue Climate Change Research Center (PCCRC) graduate fellowship program for supporting this work and the Aviation Technology Department of Purdue University, Air Transport Institute for Environmental Sustainability (AirTIES) Center, and National Test Facility for Fuels and Propulsion (NaTeF) for help collecting exhaust samples.

■ REFERENCES

(1) Logan, J. A. Nitrogen oxides in the troposphere: Global and regional budgets. *J. Geophys. Res.* **1983**, *88* (C15), 10785−10807.

DOI: 10.1021/acs.est.5b02769
Environ. Sci. Technol. XXXX, XXX, XXX−XXX

(2) Solomon, S.; Qin, D.; Manning, M.; Chen, Z.; Marquis, M.; Averyt, K. B.; Tignor, M.; Miller, H. L., Eds. Contribution of Working Group I to the Fourth Assessment Report of the Intergovernmental Panel on Climate Change. *Climate change 2007: The physical science basis*; Cambridge University Press: New York, 2007.
(3) Levy, H. Normal Atmosphere: Large Radical and Formaldehyde Concentrations Predicted. *Science* **1971**, *173* (3992), 141−143.
(4) Galloway, J. N.; Dentener, F. J.; Capone, D. G.; Boyer, E. W.; Howarth, R. W.; Seitzinger, S. P.; Asner, G. P.; Cleveland, C.; Green, P.; Holland, E.; et al. Nitrogen cycles: past, present, and future. *Biogeochemistry* **2004**, *70* (2), 153−226.
(5) Reis, S.; Pinder, R. W.; Zhang, M.; Lijie, G.; Sutton, M. A. Reactive nitrogen in atmospheric emission inventories−a review. *Atmos. Chem. Phys. Discuss.* **2009**, *9*, 12413−12464.
(6) Kim, S.-W.; Heckel, A.; Frost, G. J.; Richter, A.; Gleason, J.; Burrows, J. P.; McKeen, S.; Hsie, E.-Y.; Granier, C.; Trainer, M. NO_2 columns in the western United States observed from space and simulated by a regional chemistry model and their implications for NO_x emissions. *J. Geophys. Res.* **2009**, *114* (D11), D11301.
(7) Jaeglé, L.; Steinberger, L.; Martin, R. V.; Chance, K. Global partitioning of NO_x sources using satellite observations: Relative roles of fossil fuel combustion, biomass burning and soil emissions. *Faraday Discuss.* **2005**, *130*, 407−423.
(8) Elliott, E. M.; Kendall, C.; Wankel, S. D.; Burns, D. A.; Boyer, E. W.; Harlin, K.; Bain, D. J.; Butler, T. J. Nitrogen isotopes as indicators of NO_x source contributions to atmospheric nitrate deposition across the midwestern and northeastern United States. *Environ. Sci. Technol.* **2007**, *41* (22), 7661−7667.
(9) Elliott, E. M.; Kendall, C.; Boyer, E. W.; Burns, D. A.; Lear, G. G.; Golden, H. E.; Harlin, K.; Bytnerowicz, A.; Butler, T. J.; Glatz, R. Dual nitrate isotopes in dry deposition: Utility for partitioning NO_x source contributions to landscape nitrogen deposition. *J. Geophys. Res.* **2009**, *114* (G4), G04020.
(10) Freyer, H. D. Seasonal trends of NH_4^+ and NO_3^- nitrogen isotope composition in rain collected at Jülich, Germany. *Tellus* **1978**, *30* (1), 83−92.
(11) Felix, J. D.; Elliott, E. M. The agricultural history of human-nitrogen interactions as recorded in ice core $\delta^{15}N\text{-}NO_3^-$. *Geophys. Res. Lett.* **2013**, *40* (8), 1642−1646.
(12) Felix, J. D.; Elliott, E. M. Isotopic composition of passively collected nitrogen dioxide emissions: Vehicle, soil and livestock source signatures. *Atmos. Environ.* **2014**, *92*, 359−366.
(13) Li, D.; Wang, X. Nitrogen isotopic signature of soil-released nitric oxide (NO) after fertilizer application. *Atmos. Environ.* **2008**, *42* (19), 4747−4754.
(14) Hoering, T. The isotopic composition of the ammonia and the nitrate ion in rain. *Geochim. Cosmochim. Acta* **1957**, *12* (1−2), 97−102.
(15) Felix, J. D.; Elliott, E. M.; Shaw, S. L. Nitrogen Isotopic Composition of Coal-Fired Power Plant NO_x: Influence of Emission Controls and Implications for Global Emission Inventories. *Environ. Sci. Technol.* **2012**, *46* (6), 3528−3535.
(16) Heaton, T. H. E. $^{15}N/^{14}N$ ratios of NO_x from vehicle engines and coal-fired power stations. *Tellus B* **1990**, *42* (3), 304−307.
(17) Heaton, T. H. E. $^{15}N/^{14}N$ ratios of nitrate and ammonium in rain at Pretoria, South Africa. *Atmos. Environ.* **1987**, *21* (4), 843−852.
(18) Walters, W. W.; Goodwin, S. R.; Michalski, G. Nitrogen Stable Isotope Composition ($\delta^{15}N$) of Vehicle-Emitted NO_x. *Environ. Sci. Technol.* **2015**, *49* (4), 2278−2285.
(19) Fibiger, D. L.; Hastings, M. G.; Lew, A. F.; Peltier, R. E. Collection of NO and NO_2 for Isotopic Analysis of NO_x Emissions. *Anal. Chem.* **2014**, *86* (24), 12115−12121.
(20) Moore, H. The isotopic composition of ammonia, nitrogen dioxide and nitrate in the atmosphere. *Atmos. Environ.* **1977**, *11* (12), 1239−1243.
(21) Ammann, M.; Siegwolf, R.; Pichlmayer, F.; Suter, M.; Saurer, M.; Brunold, C. Estimating the uptake of traffic-derived NO_2 from ^{15}N abundance in Norway spruce needles. *Oecologia* **1999**, *118* (2), 124−131.
(22) Redling, K.; Elliott, E.; Bain, D.; Sherwell, J. Highway contributions to reactive nitrogen deposition: tracing the fate of vehicular NO_x using stable isotopes and plant biomonitors. *Biogeochemistry* **2013**, *116* (1−3), 261−274.
(23) Pearson, J.; Wells, D. M.; Seller, K. J.; Bennett, A.; Soares, A.; Woodall, J.; Ingrouille, M. J. Traffic exposure increases natural ^{15}N and heavy metal concentrations in mosses. *New Phytol.* **2000**, *147* (2), 317−326.
(24) Savard, M. M.; Bégin, C.; Smirnoff, A.; Marion, J.; Rioux-Paquette, E. Tree-ring nitrogen isotopes reflect anthropogenic NO_x emissions and climatic effects. *Environ. Sci. Technol.* **2009**, *43* (3), 604−609.
(25) Walters, W. W.; Michalski, G. Theoretical Calculation of Nitrogen Equilibrium Isotope Exchange Fractionation Factors for Various NO_y Molecules. *Geochim. Cosmochim. Acta* **2015**, *164*, 284−297.
(26) Freyer, H. D.; Kley, D.; Volz-Thomas, A.; Kobel, K. On the interaction of isotopic exchange processes with photochemical reactions in atmospheric oxides of nitrogen. *J. Geophys. Res.* **1993**, *98* (D8), 14791−14796.
(27) Bowman, C. T. Kinetics of pollutant formation and destruction in combustion. *Prog. Energy Combust. Sci.* **1975**, *1* (1), 33−45.
(28) Hayhurst, A. N.; Vince, I. M. Nitric oxide formation from N_2 in flames: The importance of "prompt" NO. *Prog. Energy Combust. Sci.* **1980**, *6* (1), 35−51.
(29) Toof, J. L. A Model for the Prediction of Thermal, Prompt, and Fuel NO_x Emissions From Combustion Turbines. *J. Eng. Gas Turbines Power* **1986**, *108* (2), 340−347.
(30) Heywood, J. B. Pollutant formation and control in spark-ignition engines. *Prog. Energy Combust. Sci.* **1976**, *1* (4), 135−164.
(31) Correa, S. M. A review of NO_x formation under gas-turbine combustion conditions. *Combust. Sci. Technol.* **1993**, *87* (1−6), 329−362.
(32) Maurice, L. Q.; Lander, H.; Edwards, T.; Harrison, W. E., III Advanced aviation fuels: a look ahead via a historical perspective. *Fuel* **2001**, *80* (5), 747−756.
(33) Tsague, L.; Tsogo, J.; Tatietse, T. T. Prediction of the production of nitrogen oxide in turbojet engines. *Atmos. Environ.* **2006**, *40* (29), 5727−5733.
(34) Miller, J. A.; Bowman, C. T. Mechanism and modeling of nitrogen chemistry in combustion. *Prog. Energy Combust. Sci.* **1989**, *15* (4), 287−338.
(35) Bozzelli, J. W.; Dean, A. M. O + NNH: A possible new route for NO_x formation in flames. *Int. J. Chem. Kinet.* **1995**, *27* (11), 1097−1109.
(36) Huber, K. P.; Herzberg, G. Constants of diatomic molecules. In *Molecular Spectra and Molecular Structure*; Springer: New York, 1979; pp 8−689.
(37) Taylor, K. C. Nitric oxide catalysis in automotive exhaust systems. *Catal. Rev.: Sci. Eng.* **1993**, *35* (4), 457−481.
(38) Urey, H. C. The thermodynamic properties of isotopic substances. *J. Chem. Soc.* **1947**, *7*, 562−581.
(39) Beyn, F.; Matthias, V.; Aulinger, A.; Dähnke, K. Do N-isotopes in atmospheric nitrate deposition reflect air pollution levels? *Atmos. Environ.* **2015**, *107*, 281−288.
(40) Office of Air Quality Planning and Standards. U. E. 2011 National Emissions Inventory Data & Documentation; http://www.epa.gov/ttn/chief/net/2011inventory.html (accessed Apr 16, 2015).
(41) EPA. TTN EMC Method 7 - Nitrogen Oxide (NO_x); http://www.epa.gov/ttnemc01/methods/method7.html (accessed May 6, 2015).
(42) Flamme, M. Low NO_x combustion technologies for high temperature applications. *Energy Convers. Manage.* **2001**, *42* (15−17), 1919−1935.
(43) Sigman, D. M.; Casciotti, K. L.; Andreani, M.; Barford, C.; Galanter, M.; Böhlke, J. K. A bacterial method for the nitrogen isotopic analysis of nitrate in seawater and freshwater. *Anal. Chem.* **2001**, *73* (17), 4145−4153.

DOI: 10.1021/acs.est.5b02769
Environ. Sci. Technol. XXXX, XXX, XXX−XXX

(44) Crawley, L. R. *Nitrogen and oxygen isotope-ratio analysis of nitrate by the denitrifier method using continuous flow isotope-ratio mass spectrometry*. M.S. Thesis, Purdue University, 2010.
(45) Heywood, J. B. *Internal combustion engine fundamentals*; McGraw-Hill: New York, 1988; Vol. *930*.
(46) Guzzella, L.; Onder, C. *Introduction to modeling and control of internal combustion engine systems*; Springer Science & Business Media: New York, 2009.
(47) Flagan, R. C.; Seinfeld, J. H. *Fundamentals of Air Pollution Engineering*; Prentice-Hall: Englewood Cliffs, NJ: 1988.
(48) Löffler, G.; Sieber, R.; Harasek, M.; Hofbauer, H.; Hauss, R.; Landauf, J. NO_x formation in natural gas combustion—a new simplified reaction scheme for CFD calculations. *Fuel* **2006**, *85* (4), 513−523.
(49) Smith, N. A.. *Flame Temperature Imaging of a Low NO_x Burner via Laser Rayleigh Scattering*. M.S. Thesis, Marquette University, 2009.
(50) Richet, P.; Bottinga, Y.; Javoy, M. A review of hydrogen, carbon, nitrogen, oxygen, sulphur, and chlorine stable isotope enrichment among gaseous molecules. *Annu. Rev. Earth Planet. Sci.* **1977**, *5*, 65−110.
(51) Bielaczyc, P.; Merkisz, J.; Pielecha, J. *Investigation of Exhaust Emissions from DI Diesel Engine During Cold and Warm Start*; SAE Technical Paper 2001-01-1260; SAE International: Warrendale, PA, 2001.
(52) Weilenmann, M.; Soltic, P.; Saxer, C.; Forss, A.-M.; Heeb, N. Regulated and nonregulated diesel and gasoline cold start emissions at different temperatures. *Atmos. Environ.* **2005**, *39* (13), 2433−2441.
(53) Brandenberger, S.; Kröcher, O.; Tissler, A.; Althoff, R. The State of the Art in Selective Catalytic Reduction of NO_x by Ammonia Using Metal-Exchanged Zeolite Catalysts. *Catal. Rev.: Sci. Eng.* **2008**, *50* (4), 492−531.
(54) Hu, Y.; Naito, S.; Kobayashi, N.; Hasatani, M. CO 2, NO_x and SO_2 emissions from the combustion of coal with high oxygen concentration gases. *Fuel* **2000**, *79* (15), 1925−1932.
(55) Le Bris, T.; Cadavid, F.; Caillat, S.; Pietrzyk, S.; Blondin, J.; Baudoin, B. Coal combustion modelling of large power plant, for NO_x abatement. *Fuel* **2007**, *86* (14), 2213−2220.
(56) Gerard, D.; Lave, L. B. Implementing technology-forcing policies: The 1970 Clean Air Act Amendments and the introduction of advanced automotive emissions controls in the United States. *Technol. Forecast. Soc. Change* **2005**, *72* (7), 761−778.
(57) Yan, X.; Ohara, T.; Akimoto, H. Statistical modeling of global soil NO_x emissions. *Global Biogeochem. Cycles* **2005**, *19* (3), GB3019.
(58) U.S. Energy Information Administration. Total consumption for United States, monthly; http://www.eia.gov/totalenergy/ (accessed Apr 19, 2015).

DOI: 10.1021/acs.est.5b02769
Environ. Sci. Technol. XXXX, XXX, XXX−XXX